

Fermi National Accelerator Laboratory

FERMILAB-Pub-93/069-A

CfPA-TH-93-19

astro-ph/9306029

submitted to *Physical Review D*

Tensor Perturbations in Inflationary Models as a Probe of Cosmology

Michael S. Turner,^{1,2} Martin White,³ and James E. Lidsey²

¹*Departments of Physics and of Astronomy & Astrophysics
Enrico Fermi Institute, The University of Chicago, Chicago, IL 60637-1433*

²*NASA/Fermilab Astrophysics Center, Fermi National Accelerator
Laboratory, Batavia, IL 60510-0500*

³*Center for Particle Astrophysics, University of California
Berkeley, CA 94720*

ABSTRACT

In principle, the tensor metric (gravity-wave) perturbations that arise in inflationary models can, beyond probing the underlying inflationary model, provide information about the Universe: ionization history, presence of a cosmological constant, and epoch of matter-radiation equality. Because tensor perturbations give rise to anisotropy of the cosmic background radiation (CBR) solely through the Sachs-Wolfe effect we are able to calculate analytically their contribution to the variance of the multipole moments of the CBR temperature anisotropy. In so doing, we carefully take account of the



effect of tensor perturbations that entered the Hubble radius during both the matter-dominated and radiation-dominated epoch by means of a transfer function. (Previously, only those modes that entered during the matter era were properly taken into account.) The striking feature in the spectrum of multipole amplitudes is a dramatic fall off for $l \gtrsim \sqrt{1 + z_{\text{LSS}}}$, where z_{LSS} is the red shift of the last-scattering surface, which depends upon the ionization history of the Universe. Finally, using our transfer function we provide a more precise formula for the energy density in stochastic gravitational waves from inflation, and, using the Cosmic Background Explorer Differential Microwave Radiometer (COBE DMR) quadrupole normalization, we express this energy density in terms of the “tilt” of the spectrum of tensor perturbations alone and show that it is unlikely that the stochastic background of gravity waves can be detected directly in the foreseeable future.

1 Introduction

Quantum fluctuations arising during inflation lead to a spectrum of scalar (density) [1] and tensor (gravity-wave) [2] metric perturbations which are nearly scale invariant [3]. In turn, both give rise to anisotropy in the temperature of the cosmic background radiation (CBR), with their relative contributions depending upon the steepness of the inflationary potential [4, 5]. CBR anisotropy and other astrophysical data, e.g., red-shift surveys, peculiar-velocity measurements, and data from gravity-wave detectors, can, in principle, be used to learn much about the inflationary potential in the narrow interval that governs the modes that affect astrophysically interesting scales. For example, they can be used to infer the value of the inflationary potential, its steepness and the change in its steepness [5, 6].

In all likelihood CBR anisotropy provides the cleanest and most sensitive probe of the metric perturbations created during inflation. The CBR anisotropies that arise due to scalar and gravity-wave fluctuations add incoherently and can thus be computed separately. The calculation of the anisotropy that arises due to scalar perturbations is complicated and well understood: anisotropy arises due to at least three physical effects, the Sachs-Wolfe effect [7] (gravitational potential differences on the last-scattering surface), the velocity of the last-scattering surface, and intrinsic fluctuations in the CBR temperature at last scattering. Further, the ionization history and baryon density are very important [8]. On large-angular scales, for standard recombination $\theta \gtrsim 2^\circ$, the Sachs-Wolfe effect dominates, and on small-angular scales the other two effects dominate.

The CBR anisotropy due to tensor perturbations arises solely from the Sachs-Wolfe effect. It depends significantly upon the red shift of the last-

scattering surface, and less significantly upon a possible cosmological constant and the red shift of matter-radiation equality (through the value of the Hubble constant). Thus, if the tensor contribution to CBR anisotropy can be separated from the scalar contribution, it provides a very direct probe of cosmology. The tensor contribution has been computed analytically, but only on large-angular scales with other simplifying assumptions being made [9], and recently, numerically in the case of standard recombination and a matter-dominated Universe [10].

The purpose of our paper is to give simple and accurate analytic formulae for the tensor contribution to the variance in the CBR temperature multipoles ($\langle |a_{lm}|^2 \rangle$) (“angular power spectrum”). In previous analytical work [9], only the modes that enter the horizon after matter-radiation equality were properly taken into account, so that these results are accurate only on large angular scales; we take into account the modes that enter the horizon before matter-radiation equality by means of a transfer function and thereby accurately describe the CBR anisotropy that arises on all angular scales. The transfer function also allows us to give a more precise expression for the energy density in stochastic gravity waves produced by inflation, and, unfortunately, we show that it is very unlikely that this background can be detected directly. We compare our results for CBR anisotropy, where possible, to the numerical results of Ref. [10], and discuss how the tensor multipoles depend upon the underlying cosmological parameters: the red shift of last scattering, z_{LSS} ; the red shift of matter-radiation equality, z_{EQ} ; and the presence of a cosmological constant.

2 Gravity Waves and CBR Anisotropy

2.1 Qualitative view

In this Section we begin simply and gradually add detail, ending with our most general formulae. In that spirit we will assume scale-invariant metric perturbations to begin, and then generalize our results to allow for deviation from scale invariance. For scale-invariant perturbations the amplitude of density perturbations and gravity-wave perturbations are independent of scale at horizon crossing in the post-inflationary Universe: $(\delta\rho/\rho)_{\text{HOR}} \equiv \varepsilon_S$ and $h_{\text{GW}} = \varepsilon_T$. Horizon crossing is defined by $k_{\text{phys}} = k/R \simeq H$; R is the cosmic-scale factor and H is the expansion rate. Throughout we take the scale factor to be unity at the present epoch, so that comoving wavenumber k and physical wavenumber k_{phys} are equal today; comoving wavelength λ and wavenumber are related by: $\lambda = 2\pi/k$.

It is useful to define the conformal time today, τ_0 , and at the last-scattering event, τ_{LSS} :

$$\begin{aligned}\tau_0 &= \int_0^{t_0} dt/R(t) = 2H_0^{-1}; \\ \tau_{\text{LSS}} &= \int_0^{t_{\text{LSS}}} dt/R(t) \simeq \tau_0/\sqrt{1+z_{\text{LSS}}};\end{aligned}\tag{1}$$

where we assume a flat, matter-dominated Universe today. The quantities $\tau_0 \simeq 6000h^{-1}\text{Mpc}$ and $\tau_{\text{LSS}} \simeq 6000h^{-1}\text{Mpc}/\sqrt{1+z_{\text{LSS}}}$ correspond to the comoving size of the present horizon and that at last scattering. The comoving distance to the last-scattering surface $d_{\text{LSS}} = \tau_0(1 - 1/\sqrt{1+z_{\text{LSS}}}) \simeq \tau_0$, and thus the angle subtended by the horizon scale at last scattering corresponds to $\theta_{\text{LSS}} \sim \tau_{\text{LSS}}/\tau_0$ ($\sim 2^\circ$ for $z_{\text{LSS}} = 1100$).

In the standard picture recombination occurs at a red shift of order 1300,

i.e., the ionization fraction X_e becomes small, and last-scattering occurs a red shift of about $z_{\text{LSS}} \simeq 1100$, i.e., the photon mean-free path becomes greater than the Hubble scale [11]. If the Universe remains ionized much later, or is reionized after recombination, the last-scattering event can occur much later, $1 + z_{\text{LSS}} \simeq (0.03X_e\Omega_B h)^{-2/3}$, where Ω_B is the fraction of critical density contributed by baryons, $H_0 = 100h \text{ km s}^{-1} \text{ sec}^{-1} \text{ Mpc}^{-1}$, and $\Omega_0 = 1$. Taking $h = 0.4$, $X_e = 1$, and saturating the primordial nucleosynthesis bound to the baryon mass density, $\Omega_B h^2 \lesssim 0.02$ [12], last scattering could occur as late as $z_{\text{LSS}} \simeq 76$. While the conventional wisdom has it that cold dark matter models lack a plausible mechanism for reionizing, or keeping the Universe ionized at $z \lesssim 1300$, it has been suggested that a very early generation of stars could have reionized the Universe at red shift of order 100 or so [13].

The physics underlying the Sachs-Wolfe effect is very simple: The temperature fluctuation on a given angular scale is roughly equal to the metric fluctuation on the corresponding length scale on the last-scattering surface. For tensor perturbations, the metric perturbation is equal to the gravity-wave amplitude. For scalar perturbations the metric perturbation is given by the fluctuation in the Newtonian potential; on length scales that have yet to enter the horizon at last scattering, or that entered the horizon after matter-radiation equality, the fluctuation in the Newtonian potential is given by the horizon-crossing amplitude of the density perturbation. For scales that enter the horizon while the Universe is still radiation dominated the fluctuation in the Newtonian potential decreases after horizon crossing, as R^{-1} .

The CBR temperature fluctuation that arises on a given angular scale

due to scalar perturbations through the Sachs-Wolfe effect alone is roughly:

$$\begin{aligned} \left(\frac{\delta T}{T}\right)_\theta &\sim \left(\frac{\delta\rho}{\rho}\right)_{\text{HOR},k(\theta)} \simeq \epsilon_S \quad \theta \gtrsim \theta_{\text{EQ}}; \\ \left(\frac{\delta T}{T}\right)_\theta &\sim \left(\frac{k_{\text{EQ}}}{k}\right) \left(\frac{\delta\rho}{\rho}\right)_{\text{HOR},k(\theta)} \simeq \left(\frac{\theta}{\theta_{\text{EQ}}}\right) \epsilon_S \quad \theta \lesssim \theta_{\text{EQ}}; \end{aligned} \quad (2)$$

where $k(\theta)$ corresponds to the wavelength that subtends an angle θ on the last-scattering surface,

$$k(\theta) \sim \left(\frac{200^\circ}{\theta}\right) \tau_0^{-1}. \quad (3)$$

Here, k_{EQ} is the scale that crossed the horizon at matter-radiation equality, and $\theta_{\text{EQ}} \sim 1/\sqrt{1+z_{\text{EQ}}} \sim 0.3^\circ$.

For scale-invariant perturbations and $\theta \gtrsim \theta_{\text{EQ}} \sim 0.3^\circ$, the Sachs-Wolfe contribution to the temperature fluctuation is independent of angular scale. On small-angular scales, $\theta \lesssim \theta_{\text{EQ}}$, the Sachs-Wolfe contribution to the CBR temperature anisotropy decreases, but is a subdominant contribution to total anisotropy produced by scalar perturbations. On angular scales larger than the horizon at last scattering, $\theta \gtrsim \theta_{\text{LSS}} \sim 1/\sqrt{1+z_{\text{LSS}}} (\sim 2^\circ \text{ for } z_{\text{LSS}} = 1100)$, the Sachs-Wolfe effect is the dominant contribution to CBR anisotropy.

The CBR temperature fluctuation on a given angular scale due to tensor perturbations arises solely through the Sachs-Wolfe effect and is roughly:

$$\left(\frac{\delta T}{T}\right)_\theta \sim h_{\text{GW}}[z_{\text{LSS}}, k(\theta)]; \quad (4)$$

where $h_{\text{GW}}[z_{\text{LSS}}, k(\theta)]$ is the (dimensionless) gravity-wave amplitude on the scale $k(\theta)$ at last scattering. For gravity-wave modes that have yet to re-enter the horizon at last scattering, $h_{\text{GW}}(z_{\text{LSS}}, k)$ is just equal to ϵ_T ; once a mode enters the horizon its amplitude red shifts as the scale factor, so that $h_{\text{GW}}(z_{\text{LSS}}, k) = \epsilon_T (R_{\text{HOR}}/R_{\text{LSS}})$. For modes that enter the horizon during

the matter-dominated epoch, $R_{\text{HOR}}/R_{\text{LSS}} \simeq (k\tau_{\text{LSS}})^{-2}$; for modes that enter during the radiation-dominated epoch, $R_{\text{HOR}}/R_{\text{LSS}} \simeq (k/k_{\text{EQ}})(k\tau_{\text{LSS}})^{-2}$. [A simple way to understand why the amplitude of a gravity-wave mode red shifts as the scale factor after it enters the horizon is that gravity-wave perturbations correspond to massless bosons (gravitons) whose energy density ($\propto m_{\text{Pl}}^2 k_{\text{phys}}^2 h_{\text{GW}}^2$) red shifts as R^{-4} .]

For scale-invariant tensor perturbations the CBR anisotropy due to gravity waves is only independent of scale for $\theta \gtrsim \theta_{\text{LSS}}$; on smaller angular scales it decreases,

$$\begin{aligned}
 \left(\frac{\delta T}{T}\right)_{\theta} &\sim \epsilon_T & \theta &\gtrsim \theta_{\text{LSS}}; \\
 \left(\frac{\delta T}{T}\right)_{\theta} &\sim \epsilon_T \left(\frac{\theta}{\theta_{\text{LSS}}}\right)^2 & \theta_{\text{LSS}} &\gtrsim \theta \gtrsim \theta_{\text{EQ}}; \\
 \left(\frac{\delta T}{T}\right)_{\theta} &\sim \epsilon_T \left(\frac{\theta\theta_{\text{EQ}}}{\theta_{\text{LSS}}^2}\right) & \theta &\lesssim \theta_{\text{EQ}}.
 \end{aligned} \tag{5}$$

On angular scales greater than that subtended by the horizon at last scattering, $\theta_{\text{LSS}} \sim 2^\circ$ in the standard scenario, the ratio of the tensor to the scalar contributions to the temperature anisotropy is constant and equal to ϵ_T/ϵ_S ; in turn, this ratio is related to the steepness of the inflationary potential, evaluated when these scales crossed outside the horizon during inflation (about 50 e-folds before the end of inflation): $\epsilon_T/\epsilon_S \sim x_{50} \equiv (m_{\text{Pl}}V'/V)_{50}$ [4]. On smaller angular scales the tensor contribution falls as θ^2 because these scales are dominated by gravity-wave modes that have entered the horizon before the epoch of last scattering and have had their amplitudes red shifted. On the smallest angular scales the tensor contribution only decreases as θ , as these scales are dominated by gravity-wave modes that enter the horizon before matter radiation equality. The steep fall off of gravity-wave modes for

$l \gtrsim \sqrt{1 + z_{\text{LSS}}}$ provides a potential signature of z_{LSS} and tensor perturbations.

It is conventional to expand the CBR temperature fluctuation on the sky in spherical harmonics:

$$\frac{\delta T(\hat{\mathbf{x}})}{T_0} = \sum_{l=2}^{\infty} \sum_{m=-l}^l a_{lm}(\mathbf{r}) Y_{lm}(\hat{\mathbf{x}}); \quad (6)$$

where the unobservable monopole term and the dipole term, which is dominated by the contribution of the observer's peculiar velocity, are omitted. The multipole amplitudes depend upon the observer's position \mathbf{r} . The quantity $|a_{lm}|^2$ averaged over all observation positions (the ensemble average) is referred to as the angular power spectrum,¹ and is related approximately to the CBR temperature fluctuation by

$$\left(\frac{\delta T}{T}\right)_\theta^2 \sim l^2 \langle |a_{lm}|^2 \rangle \quad \text{for } l \sim 200^\circ/\theta. \quad (7)$$

To be more precise, the *rms* temperature fluctuation averaged over the sky for a given experiment is given by

$$\left\langle \left(\frac{\delta T}{T_0}\right)^2 \right\rangle = \sum_{l \geq 2} \frac{2l+1}{4\pi} \langle |a_{lm}|^2 \rangle W_l; \quad (8)$$

where W_l is the appropriate response function for the experiment. For a two-beam experiment, where the temperature difference between two antennas of gaussian beam width σ separated by angle θ is measured,

$$W_l = 2 [1 - P_l(\cos \theta)] e^{-(l+1/2)^2 \sigma^2}.$$

For scale-invariant density perturbations the Sachs-Wolfe contribution to l^2 times the angular power spectrum is roughly constant and equal to ϵ_S

¹More precisely, the average is over all realizations of the fluctuation spectrum; we have implicitly assumed spatial ergodicity.

for $l \lesssim l_{\text{EQ}}$; thereafter it decreases as l^{-2} . For scale-invariant gravity-wave perturbations l^2 times the angular power spectrum is constant for $l \lesssim l_{\text{LSS}}$ (~ 30 for standard recombination); it decreases as l^{-4} for $l \lesssim l_{\text{EQ}}$; and as l^{-2} for $l \gtrsim l_{\text{EQ}}$.

Finally, if the scalar and tensor perturbations are “tilted”—that is not scale invariant—say $\varepsilon_S \propto \lambda^{\alpha_S}$ and $\varepsilon_T \propto \lambda^{\alpha_T}$, the previous results for $(\delta T/T)_\theta$ are modified by factors of θ^{α_S} and θ^{α_T} respectively, and for $\langle |a_{lm}|^2 \rangle$, by factors of $l^{-2\alpha_S}$ and $l^{-2\alpha_T}$ respectively. The quantities α_S and α_T are related to the power-law indices often used to characterize the scalar and tensor perturbations (see below) by

$$\alpha_S = (1 - n)/2; \quad \alpha_T = -n_T/2.$$

The qualitative behaviour of the CBR anisotropy due to scalar and tensor perturbations is shown in Fig. 1.

2.2 Quantitative view

Some of what follows is a quick review of previous treatments included for completeness; for more details see Refs. [9]. To begin, we write the line element for a flat, Friedmann-Robertson-Walker (FRW) cosmology in conformal form plus a small perturbation $h_{\mu\nu}$:

$$g_{\mu\nu} = R^2(\tau)[\eta_{\mu\nu} + h_{\mu\nu}], \quad (9)$$

where $\eta_{\mu\nu} = \text{diag}(1, -1, -1, -1)$ and τ is conformal time. Here we are only interested in gravity-wave perturbations and work in the transverse-traceless gauge, where the two independent polarization states are \times and $+$, and $h_{00} = h_{0j} = 0$.

It is simple to solve for the evolution of the cosmic-scale factor in terms of conformal time:

$$R(\tau) = \left[\tau/\tau_0 + R_{\text{EQ}}^{1/2} \right]^2 - R_{\text{EQ}}; \quad (10)$$

where we have assumed a flat Universe with matter and radiation (i.e., photons with present temperature 2.726 K and three massless neutrino species), $R_0 = 1$, $\tau_0 = 2H_0^{-1} \sqrt{1 + R_{\text{EQ}}} \simeq 2H_0^{-1}$, $R_{\text{EQ}} = 4.18 \times 10^{-5} h^{-2}$ is the value of the cosmic scale factor at the epoch of matter-radiation equality, and $\tau_{\text{EQ}} = [\sqrt{2} - 1] R_{\text{EQ}}^{1/2} \tau_0$. (The conformal age of the Universe today differs from $2H_0^{-1}$ by a small amount due to the tiny contribution of the radiation energy density today:

$$\tau_{\text{today}} = \tau_0 \left[\sqrt{1 + R_{\text{EQ}}} - \sqrt{R_{\text{EQ}}} \right] \simeq 2H_0^{-1} \left(1 - \sqrt{R_{\text{EQ}}} \right) \approx 2H_0^{-1} [1 - \mathcal{O}(1\%)],$$

which we shall henceforth neglect.)

We expand the gravity-wave perturbation in plane waves

$$h_{jk}(\mathbf{x}, \tau) = (2\pi)^{-3} \int d^3k h_{\mathbf{k}}^i(\tau) \epsilon_{jk}^i e^{-i\mathbf{k}\cdot\mathbf{x}}; \quad (11)$$

where ϵ_{jk}^i is the polarization tensor and $i = \times, +$. The gravity-wave perturbation satisfies the massless Klein-Gordon equation

$$\ddot{h}_{\mathbf{k}}^i + 2 \left(\frac{\dot{R}}{R} \right) \dot{h}_{\mathbf{k}}^i + k^2 h_{\mathbf{k}}^i = 0; \quad (12)$$

where an overdot indicates a derivative with respect to conformal time and $k^2 = \mathbf{k} \cdot \mathbf{k}$.

The growing-mode solutions to this equation have simple qualitative behaviour: before horizon crossing ($k\tau \ll 1$) $h_{\mathbf{k}}^i(\tau)$ is constant; well after horizon crossing ($k\tau \gg 1$) $h_{\mathbf{k}}^i \propto \cos k\tau/R$. For modes that cross inside the horizon during the radiation-dominated era the exact solution prior to and

including the radiation-dominated era is $j_0(k\tau)$; for modes that cross inside the horizon during the matter-dominated era the exact solution is $3j_1(k\tau)/k\tau$. Here $j_0(z) = \sin z/z$ and $j_1(z) = \sin z/z^2 - \cos z/z$ are the spherical-Bessel functions of order zero and one respectively, and both Bessel-function solutions have been normalized to unity for $\tau \rightarrow 0$.

Well into the matter-dominated era the temporal behaviour of modes that entered the horizon during the radiation-dominated era is also given by $3j_1(k\tau)/k\tau$. Thus, for $\tau \gg \tau_{\text{EQ}}$ the temporal behaviour of *all* modes is given by $3j_1(k\tau)/k\tau$, and it is useful to write

$$h_{\mathbf{k}}^i(\tau) = h_{\mathbf{k}}^i(0) T(k/k_{\text{EQ}}) \left(\frac{3j_1(k\tau)}{k\tau} \right); \quad (13)$$

where the “transfer function” for gravitational waves, $T(k/k_{\text{EQ}})$, is only a function of k/k_{EQ} , and

$$k_{\text{EQ}} \equiv \tau_{\text{EQ}}^{-1} = \frac{\tau_0^{-1} R_{\text{EQ}}^{-1}}{\sqrt{2} - 1} \simeq 6.22 \times 10^{-2} h^2 \text{Mpc}^{-1}; \quad (14)$$

is the scale that entered the horizon at matter-radiation equality. Note, during the oscillatory phase ($k\tau \gg 1$), $3j_1(k\tau)/k\tau \rightarrow 3 \cos k\tau/(k\tau)^2$; in defining and computing the transfer function we have neglected the phase of the graviton oscillations, which, for our purposes, is not important.

The transfer function has been calculated by integrating Eq. (13) numerically from $\tau = 0$ to $\tau = \tau_0$; a good fit to the transfer function is

$$T(y) = [1.0 + 1.34y + 2.50y^2]^{1/2}; \quad (15)$$

where $y = k/k_{\text{EQ}}$. It might seem that one could have computed the transfer function at any time after the Universe becomes matter dominated and obtained the same result. However, as we shall emphasize again later, the

Universe becomes matter dominated more slowly than one might have expected, and for this reason the transfer function calculated at an earlier epoch is different. Only well into the matter-dominated epoch, when the radiation content is very negligible, does it take this functional form. Using the fact that once a mode is well inside the horizon $h_{\mathbf{k}}^i(\tau) \propto \cos k\tau/R$ it follows that for modes with $k \gg k_{\text{EQ}}$ the transfer function at an earlier epoch is related to that today by

$$T_{\tau}(k/k_{\text{EQ}}) = (\tau/\tau_0)^2 R^{-1} T(k/k_{\text{EQ}}) = [1 + 2x - 2\sqrt{x + x^2}] T_0(k/k_{\text{EQ}}); \quad (16)$$

where $x = R_{\text{EQ}}/R(\tau)$, T_{τ} is the transfer function at conformal time τ , and T is the transfer function today. The evolution of the transfer function is shown in Fig. 2.

Once a mode has crossed inside the horizon one can sensibly talk about the corresponding energy density in gravitons; it is given by

$$k \frac{d\rho_i}{dk} = \frac{m_{\text{Pl}}^2 k^5}{32\pi^3 R^2} \overline{|h_{\mathbf{k}}^i(\tau)|^2}; \quad (17)$$

where $\overline{|h_{\mathbf{k}}^i|^2}$ is the average of $|h_{\mathbf{k}}^i|^2$ over all directions $\hat{\mathbf{k}}$ and over several periods.

Inflation-produced tensor perturbations are stochastic in nature and characterized by a gaussian random variable. The Fourier components $h_{\mathbf{k}}^i$ are drawn from a distribution whose statistical expectation is

$$\langle h_{\mathbf{k}}^i h_{\mathbf{q}}^j \rangle = P_T(k) (2\pi)^6 \delta^{(3)}(\mathbf{k} - \mathbf{q}) \delta_{ij}; \quad (18)$$

where we define the gravity-wave power spectrum as²

$$P_T(k) = A_T k^{-3} |T(k)|^2 \left[\frac{3j_1(k\tau)}{k\tau} \right]^2$$

²Our notation is by no means standard; cf. [9].

$$A_T = \frac{8}{3\pi} \frac{V_{50}}{m_{\text{Pl}}^4}. \quad (19)$$

The quantity V_{50} is the value of the scalar potential around 50 e-folds before the end of inflation when the modes of astrophysical interest, say $\lambda \sim 1 \text{ Mpc} - 10^4 \text{ Mpc}$, were excited and crossed outside the horizon; see [5]. [We note that the ensemble average and power spectrum are related by, $\langle |h_{\mathbf{k}}^i|^2 \rangle = (2\pi)^3 P_T(k)$.]

Using Eqs. (18, 19) it is a simple matter to compute the energy density today in the stochastic gravitational-wave background produced by inflation:

$$\frac{d\Omega_{\text{GW}}}{d \ln k} \equiv \sum_i \frac{k}{\rho_{\text{crit}}} \frac{d\rho_i}{dk} = 4 \frac{V_{50}}{m_{\text{Pl}}^4} |T(k/k_{\text{EQ}})|^2 (k\tau_0)^{-2}; \quad (20)$$

where $\rho_{\text{crit}} = 3H_0^2/8\pi G \simeq 1.05h^2 \times 10^4 \text{ eV cm}^{-3}$ is the present value of the critical density. This agrees with previous results [14] in the limit $k \ll k_{\text{EQ}}$, and is shown in Fig. 3.

The spectrum of gravitational waves is cut off at wavenumber [14]

$$k_{\text{max}} \approx \frac{T_0 (\mathcal{M}^2 T_{\text{RH}})^{1/3}}{m_{\text{Pl}}} \sim 10^{21} \left(\frac{\mathcal{M}}{10^{14} \text{ GeV}} \right)^{2/3} \left(\frac{T_{\text{RH}}}{10^{14} \text{ GeV}} \right)^{1/3} \text{ Mpc}^{-1}; \quad (21)$$

where \mathcal{M}^4 is the vacuum energy at the very end of inflation, T_{RH} is the reheat temperature, and $T_0 = 2.726 \text{ K}$ is the present temperature. The scale k_{max} corresponds to the scale that crossed outside the horizon just as inflation ended, and is the highest frequency gravity wave produced.

If 100% of the vacuum energy is converted into radiation at reheating, then inflation is followed immediately by the usual radiation-dominated epoch and $T_{\text{RH}} \simeq \mathcal{M}$. For “imperfect reheating,” there is an epoch between the end of inflation and the beginning of radiation domination where the energy density of the Universe is dominated by the coherent oscillations of the

scalar field responsible for inflation, and $T_{\text{RH}} < \mathcal{M}$. In this case, the energy density in gravitational waves decreases as k^{-2} from $k = k_* \approx T_0 (T_{\text{RH}}/m_{\text{Pl}})$ to $k = k_{\text{max}}$ [3]; the scale k_* crossed back inside the horizon just as the Universe became radiation dominated.

The contribution of tensor perturbations to the variance of the multipoles, which arises solely through the Sachs-Wolfe effect [7, 9], is given by

$$\langle |a_{lm}|^2 \rangle = 36\pi^2 A_T \frac{\Gamma(l+3)}{\Gamma(l-1)} \int_0^\infty |F_l(u)|^2 |T(u/u_{\text{EQ}})|^2 \frac{du}{u}; \quad (22)$$

where

$$F_l(u) = - \int_{(\tau_{\text{SS}}/\tau_0)u}^u dy \left(\frac{j_2(y)}{y} \right) \left[\frac{j_l(u-y)}{(u-y)^2} \right], \quad (23)$$

$u = k\tau_0$, $y = k\tau$, and $u_{\text{EQ}} = k_{\text{EQ}}\tau_0$.

This expression is identical to previous results with the exception of the inclusion of the transfer function to properly take account of short-wavelength modes, $k \gtrsim k_{\text{EQ}}$. Since $|T(k/k_{\text{EQ}})|^2 \propto k^2$ for $k \gtrsim k_{\text{EQ}}$, without the transfer function the contribution from these modes has been *underestimated*. In Fig. 4 we show our results for the variance of the multipole moments, compared to those which do not take the short-wavelength modes into account properly. The correction to previous results is important even for values of l as small as 10 or so.

The tensor contribution to the quadrupole CBR temperature anisotropy is given by

$$\left(\frac{\Delta T}{T_0} \right)_{Q-T}^2 \equiv \frac{5\langle |a_{2m}|^2 \rangle}{4\pi} \simeq 0.606 \frac{V_{50}}{m_{\text{Pl}}^4}; \quad (24)$$

where the integrals in the previous expressions have been evaluated numerically; for the quadrupole term, including the transfer function does not make a significant difference. Using the COBE DMR measurement for the quadrupole anisotropy (derived for scale-invariant perturbations),

$\Delta T_Q = 17 \pm 4 \mu\text{K}$ [15], as a rough upper limit to the tensor contribution, V_{50} can be bounded [16],

$$V_{50} \lesssim 6.4 \times 10^{-11} m_{\text{Pl}}^4 \simeq (3.5 \times 10^{16} \text{ GeV})^4. \quad (25)$$

This implies that inflation takes place at a subPlanck energy scale (at least the last 50 or so e-folds that are relevant for us) and that Ω_{GW} can be at most about 10^{-10} . In models of first-order inflation another, more potent, source of gravity waves is produced by bubble collisions during reheating, though this radiation is peaked over a very narrow range of frequencies, $k \approx 2 \times 10^{21} (T_{\text{RH}}/10^{14} \text{ GeV}) \text{ Mpc}^{-1}$ [17].

For reference, the Sachs-Wolfe contribution to the CBR anisotropy produced by scalar modes, which is the dominant contribution for $l \lesssim 100$, is

$$\begin{aligned} \langle |a_{lm}|^2 \rangle &= A \frac{H_0^4}{2\pi} \int_0^\infty |T_S(u/u_{\text{EQ}})|^2 |j_l(u)|^2 \frac{du}{u}; \\ A &= \frac{1024\pi^3}{75H_0^4} \frac{V_{50}}{m_{\text{Pl}}^4 x_{50}^2}; \\ \left(\frac{\Delta T}{T_0}\right)_{Q-S}^2 &\equiv \frac{5\langle |a_{2m}|^2 \rangle}{4\pi} \approx \frac{32\pi}{45} \frac{V_{50}}{m_{\text{Pl}}^4 x_{50}^2}; \end{aligned} \quad (26)$$

where $u = k\tau_0$, $u_{\text{EQ}} = k_{\text{EQ}}$, and $T_S(y)$ is the transfer function for scalar perturbations, which depends upon the matter content of the Universe. For cold dark matter the transfer function is [18]

$$T_S(y) = \frac{\ln(1 + 0.146y)/0.146y}{[1 + 0.242y + y^2 + (0.340y)^3 + (0.417y)^4]^{1/4}}. \quad (27)$$

The scalar and tensor contributions to a given multipole are dominated by wavenumbers $k\tau_0 \approx l$. For scale-invariant perturbations and small l , both the scalar and tensor contributions to $l^2 \langle |a_{lm}|^2 \rangle$ are approximately constant. The Sachs-Wolfe contribution of scalar perturbations to $l^2 \langle |a_{lm}|^2 \rangle$ begins to

decrease for $l = l_{\text{EQ}} \sim 100$ since the scalar contribution to these multipoles is dominated by modes that entered the horizon before matter domination and are suppressed by the (scalar) transfer function. (It is important to remember that for $l \gtrsim 100$ the Doppler and intrinsic contributions to the scalar-produced CBR anisotropy dominate.) The contribution of tensor modes to $l^2 \langle |a_{lm}|^2 \rangle$ begins to decrease for $l \sim \tau_0 / \tau_{\text{LSS}} \approx \sqrt{1 + z_{\text{LSS}}} (\sim 35$ for $z_{\text{LSS}} \sim 1100)$ because the tensor contribution to these multipoles is dominated by modes that entered the horizon before last scattering (and hence decayed as R^{-1} until last scattering). The behaviour of the multipole amplitudes is just as expected from the qualitative picture, cf. Fig. 1, and is illustrated in Fig. 4.

2.3 Finite thickness of the last-scattering surface

Last scattering is not an instantaneous event that occurred simultaneously everywhere in the Universe. The last-scattering surface has a finite thickness, in comoving distance from the observer, σ_x , and in red shift, σ_z . This fact leads to the damping of the contribution of modes with large wavenumber because the contribution to CBR anisotropy in a given direction averages over last-scattering events taking place over a finite distance, which washes out short-wavelength modes, $k \gtrsim k_D = \sigma_x^{-1}$. *This physics is not included in our analysis.* Since the l th multipole is dominated by the contribution of wavenumbers $k\tau_0 \approx l$, this damping only affects multipoles $l \gtrsim \tau_0 / \sigma_x$, multipoles that were already very small. Thus, our neglect of the finite thickness of the last-scattering surface does not affect our results in an important way. (This is not true for scalar perturbations: the finite thickness of the last-scattering surface reduces the CBR anisotropy on small-angular scales that

would otherwise be large.)

To be more specific, in the case of standard recombination, the differential probability that the last-scattering event occurred at comoving distance x —the visibility function—can be approximated by a gaussian (see e.g., [11])

$$\frac{d\mathcal{P}}{dx} \equiv \frac{ds}{dx} e^{-s(x)} \simeq C \exp[-(x - x_{\text{LSS}})^2/2\sigma_x^2], \quad (28)$$

where $C \simeq 182H_0$, $x_{\text{LSS}} \simeq 2H_0^{-1}$ is the center of the last-scattering surface, and $\sigma_x = 2H_0^{-1}/910$ is the thickness of the last-scattering surface. (In red shift, the thickness is $\sigma_x \simeq 80$.) Here $s(x)$ is the optical depth from our position to a point comoving distance x from us,

$$s(x) = \int_0^x n_e(x) \sigma_T \frac{dt}{dx} dx, \quad (29)$$

where $\sigma_T \simeq 0.66 \times 10^{-24} \text{cm}^2$ is the Thomson cross section and n_e is the number density of free electrons ($\approx X_e n_B$). The damping scale associated with the thickness of the last-scattering surface is $k_D \tau_0 = \tau_0/\sigma_x \simeq 910$, which leads to the suppression of the angular power spectrum for $l \gtrsim 910$, where it is already very small, cf. Fig. 4.

In the case of no, or only partial, recombination the last-scattering surface is very thick, $\sigma_x \sim z_{\text{LSS}}$. The visibility function can be (less well) approximated by a gaussian,

$$\frac{d\mathcal{P}}{dx} \simeq C \exp[-(x - x_{\text{LSS}})^2/2\sigma_x^2], \quad (30)$$

where

$$C = 1/\sqrt{2\pi}\sigma_x; \quad x_{\text{LSS}} \simeq 2H_0^{-1}[1 - 1/\sqrt{1 + z_{\text{LSS}})]; \quad \sigma_x \simeq 2H_0^{-1}\sqrt{12(1 + z_{\text{LSS}})}.$$

The red shift of the last-scattering surface

$$1 + z_{\text{LSS}} \simeq (0.03X_e\Omega_B h)^{-2/3}.$$

In the case of nonstandard recombination the damping scale $k_D\tau_0 \simeq 4\sqrt{z_{\text{LSS}}}$ is smaller—because the last-scattering surface is thicker—but again, this damping only affects multipoles that were very small anyway, $l \gtrsim 4\sqrt{z_{\text{LSS}}} \gg \sqrt{z_{\text{LSS}}}$, cf. Fig. 5.

2.4 Comparison with numerical results

In Ref. [10] the coupled Boltzmann equations for the CBR intensity in a perturbed FRW model were solved numerically to compute the CBR anisotropy that arises due to both scalar and tensor perturbations. The authors of Ref. [10] have graciously about comparing their preliminary results with ours. Where comparison is possible, the agreement is always qualitatively very good, though there are quantitative disagreements: for values of l where the multipoles are of significant size at most about 20%. As we shall describe, we believe that we understand the reason for these disagreements.

For very large l , corresponding to $l \gtrsim k_D\tau_0$, the numerical results of Ref. [10] fall off more rapidly than ours; as discussed above this is because we have not taken account of the damping due to the finite thickness of the last scattering surface. The discrepancy here—though large—is of little practical concern as the multipoles are very small for such values of l .

A more important discrepancy arises in cases where last-scattering occurs before the Universe is “very matter dominated.” The matter and radiation energy densities become equal at a red shift $z_{\text{EQ}} \simeq 2.4h^2 \times 10^4$; for $h = 0.5$ and standard recombination z_{LSS} and z_{EQ} differ only by a factor of 5.4. This means that the Universe is not well approximated as being matter dominated at last scattering. In particular, the growing mode gravity-wave perturbation

is not given by $3j_1(k\tau)/k\tau$ and

$$\tau_{\text{LSS}} = 2H_0^{-1} \left(1 + \sqrt{R_{\text{EQ}}}\right) \left[\sqrt{R_{\text{LSS}} + R_{\text{EQ}}} - \sqrt{R_{\text{EQ}}}\right],$$

which differs from the matter-dominated result, $\tau_{\text{LSS}} = 2H_0^{-1}\sqrt{R_{\text{LSS}}}$ by a factor of 2/3. To correct Eq. (23) one would have to: (i) Use the correct expression for τ_{LSS} , which is easy to do; (ii) Modify the transfer function, taking into account that it is a function of red shift, which means that it can no longer be taken out of the inner integral; and (iii) Replace the conformal-time derivative of the growing-mode eigenfunction, the $j_2(y)/y$ term, by the proper expression which must be evaluated numerically and is a separate function of τ and k (points (ii) and (iii) are not unrelated). Needless to say, these modifications eliminate the advantages of the analytic approach.

The parameter that controls the size of the error made by assuming that the Universe is matter dominated at last-scattering is $z_{\text{LSS}}/z_{\text{EQ}}$. In the worst case considered, standard recombination and $h = 0.5$, this parameter is about 0.2, which is about equal to the maximum difference between our analytical results and the numerical results of Ref. [10]. When $z_{\text{LSS}}/z_{\text{EQ}}$ is smaller, e.g., larger Hubble constant or nonstandard recombination, the discrepancy is much smaller. For example, with $h = 0.5$ and $z_{\text{LSS}} = 76$, the differences between the numerical results of Ref. [10] and our analytical results is only a few per cent (until the multipoles become very small due to the damping associated with the finite thickness of the last-scattering surface). The advantage of the analytic approach is ease of calculation, particularly the ability to study a variety of scenarios.

2.5 Generalized for tilt

We now extend our results to the general case where the inflationary perturbations are not precisely scale invariant. Since the ratio of the tensor to scalar contribution to the CBR quadrupole anisotropy increases with tilt, $\langle |a_{2m}^T|^2 \rangle / \langle |a_{2m}^S|^2 \rangle \approx -7n_T$ ($n_T = 0$ for scale invariance), the case of non scale-invariant perturbations is very relevant in discussing tensor perturbations. The deviations from scale invariance are most significant for steep potentials (e.g., exponential potentials) and potentials whose steepness changes rapidly (e.g., low-order polynomial potentials). To lowest order in the deviation from scale invariance everything can be expressed in terms of the value of the potential V_{50} , its steepness $x_{50} = (m_{\text{Pl}} V' / V)_{50}$, and the change in its steepness x'_{50} , all evaluated about 50 e-folds before the end of inflation where the scales of astrophysical interest crossed outside the horizon during inflation [5, 19].

Beginning with the tensor perturbations and using our previous notation, the power spectrum is now given by

$$\begin{aligned}
 P_T(k) &= A_T k^{n_T-3} |T(k/k_{\text{EQ}})|^2 \left[\frac{3j_1(k\tau)}{k\tau} \right]^2; \\
 A_T &= \frac{8}{3\pi} \frac{V_{50}}{m_{\text{Pl}}^4} \frac{[\Gamma(\frac{3}{2} - \frac{1}{2}n_T)]^2}{(1 - \frac{5}{6}n_T)2^{n_T}[\Gamma(\frac{3}{2})]^2} k_{50}^{-n_T}; \\
 n_T &= -\frac{x_{50}^2}{8\pi}.
 \end{aligned} \tag{31}$$

Here k_{50} is the scale that crossed outside the horizon 50 e-folds before the end of inflation, n_T measures the deviation from scale invariance, and the expression for A_T includes the $\mathcal{O}(n_T)$ correction. (All formulas simplify if the potential and its derivatives are evaluated at the point where the present horizon scale crossed outside the horizon, i.e., $k_{50}\tau_0 \approx 1$.) The variance of

the multipole amplitudes is given by

$$\langle |a_{lm}|^2 \rangle = 36\pi^2 A_T \frac{\Gamma(l+3)}{\Gamma(l-1)} \tau_0^{-n_T} \int_0^\infty u^{n_T} |T(u/u_{\text{EQ}})|^2 |F_l(u)|^2 \frac{du}{u}; \quad (32)$$

where $F_l(u)$ is defined in Eq. (24), $u = k\tau_0$, $y = k\tau$, and $u_{\text{EQ}} = k_{\text{EQ}}\tau_0$.

In Fig. 6 we show the scalar and tensor contributions to the angular power spectrum for spectra that are tilted by the same amount, $n-1 = n_T = -0.15$. This is an interesting case because the scalar and tensor contributions to the quadrupole anisotropy are essentially equal [4]. The effect of scale noninvariance is to tilt the angular power spectra, by approximately a factor of l^{n-1} for scalar and l^{n_T} for tensor.

The analogous expressions for scalar perturbations are

$$\begin{aligned} A &= \frac{1024\pi^3}{75H_0^{3+n}} \frac{V_{50}}{m_{\text{Pl}}^4 x_{50}^2} \frac{\left\{ \Gamma\left[\frac{3}{2} - \frac{1}{2}(n-1)\right] \right\}^2}{\left[1 + \frac{7}{6}n_T - \frac{1}{3}(n-1)\right] 2^{n-1} \left[\Gamma\left(\frac{3}{2}\right)\right]^2} k_{50}^{1-n}; \\ n &= 1 - \frac{x_{50}^2}{8\pi} + \frac{m_{\text{Pl}} x'_{50}}{4\pi}; \\ \langle |a_{lm}|^2 \rangle &= A \frac{H_0^4}{2\pi} \tau_0^{1-n} \int_0^\infty u^{n-1} |T_S(u/u_{\text{EQ}})|^2 |j_l(u)|^2 \frac{du}{u}; \end{aligned} \quad (33)$$

where $u = k\tau_0$, $u_{\text{EQ}} = k_{\text{EQ}}$, and $T_S(u/u_{\text{EQ}})$ is the transfer function for scalar perturbations.

By numerically integrating Eqs. (33,34) we obtain approximate expressions for the quadrupole anisotropy due to scalar and tensor perturbations in the non scale-invariant case:

$$\begin{aligned} \frac{5\langle |a_{lm}^S|^2 \rangle}{4\pi} &= 2.22 \frac{V_{50}}{m_{\text{Pl}}^4 x_{50}^2} \left(1 + 1.1(n-1) + \frac{7}{6}[n_T - (n-1)] \right); \\ \frac{5\langle |a_{lm}^T|^2 \rangle}{4\pi} &= 0.606 \frac{V_{50}}{m_{\text{Pl}}^4} (1 + 1.2n_T); \\ \frac{\langle |a_{2m}^T|^2 \rangle}{\langle |a_{2m}^S|^2 \rangle} &\simeq -7n_T (1 + 1.1n_T + 0.1[n_T - (n-1)]). \end{aligned} \quad (34)$$

We have taken $k_{50}\tau_0 = 1$, $z_{\text{LSS}} = 1100$ (the results change very little for $z_{\text{LSS}} = 76$), and for the scalar case $h = 0.5$. Using these expressions, the fact that the scalar and tensor contributions to the quadrupole anisotropy add incoherently, and the COBE DMR quadrupole measurement, we can solve for the variance of the tensor quadrupole, equivalently V_{50}/m_{Pl}^4 , in terms of the tensor tilt n_T :

$$\begin{aligned} \langle |a_{2m}^T|^2 \rangle &\simeq \frac{9.8 \times 10^{-11}}{1 - 0.14n_T^{-1}}; \\ \frac{V_{50}}{m_{\text{Pl}}^4} &\simeq \frac{6.4 \times 10^{-11}}{1 - 0.14n_T^{-1}}. \end{aligned} \quad (35)$$

These expressions indicate that the more tilted the gravity-wave spectrum is, the larger is its amplitude, as noted earlier [4].

The energy density in the stochastic background of inflation-produced gravitational waves today is given by

$$\begin{aligned} \frac{d\Omega_{\text{GW}}}{d \ln k} &= 4 \frac{V_{50}}{m_{\text{Pl}}^4} \frac{[\Gamma(\frac{3}{2} - \frac{1}{2}n_T)]^2}{(1 - \frac{5}{6}n_T)2^{n_T}[\Gamma(\frac{3}{2})]^2} (k/k_{50})^{n_T} |T(k/k_{\text{EQ}})|^2 (k\tau_0)^{-2}; \\ &\simeq \frac{2.6 \times 10^{-10}}{1 - 0.14n_T^{-1}} (1 + 0.1n_T) (k/k_{50})^{n_T} |T(k/k_{\text{EQ}})|^2 (k\tau_0)^{-2}; \end{aligned} \quad (36)$$

where the second expression follows from using the COBE DMR normalization to express the energy density in gravity waves in terms of the tilt parameter n_T alone. In Fig. 3 we show the spectrum of stochastic gravitational waves for $n_T = -0.003, -0.03, -0.3$, using the COBE quadrupole normalization.

The total energy density in gravity waves increases with tilt (i.e., $n_T < 0$), as does the tensor contribution to the CBR quadrupole anisotropy. However, this is not the entire story; the most sensitive ‘‘direct’’ probes of gravity waves, millisecond pulsars [20] and future Laser Interferometer Gravity-wave

Observatories (LIGOs) [21], are only sensitive to gravity waves with very large wavenumber, $k\tau_0 \equiv e^N$ with $N \sim 26$ for millisecond pulsars and $N \sim 48$ for envisaged LIGO detectors. Because of the $(k/k_{50})^{n_T}$ factor in Eq. (37) tilt depresses the energy density in gravity waves on the relevant scales. To be more specific, for $k \gg k_{\text{EQ}}$ and $h = 0.5$

$$\frac{d\Omega_{\text{GW}}(k = e^N \tau_0^{-1})}{d \ln k} \simeq 1.9 \times 10^{-14} \frac{n_T e^{n_T N}}{n_T - 0.14}. \quad (37)$$

It is simple to show that the energy density in gravity waves on the scale $k = e^N \tau_0^{-1}$ is *maximized* for a value of $n_T \approx -1/N$, at a value of about $5 \times 10^{-14}/N$. While the amount of tilt that maximizes the energy density in gravity waves on the scales relevant to both millisecond pulsars, $n_T \simeq -0.04$, and LIGOs, $n_T \simeq -0.02$, is quite reasonable in the context of well motivated inflationary models [5], the predicted energy density in gravity waves is well below the sensitivity of either detector, about $\Omega_{\text{GW}} \sim 10^{-10}$ for advanced LIGO detectors and $\sim 10^{-7}$ currently for millisecond pulsars. Thus, direct detection of the stochastic background of gravitational waves does not seem promising.

3 Discussion

The tensor contribution to the variance of the multipole amplitudes depends significantly upon the red shift of the last-scattering surface and less importantly upon the red shift of matter-radiation equality through the value of the Hubble constant (see Fig. 4). For scale-invariant gravity-wave perturbations $l^2 \langle |a_{lm}|^2 \rangle$ is roughly constant for $l \lesssim \sqrt{1 + z_{\text{LSS}}}$; then decreases as l^{-4} for $l \lesssim \sqrt{1 + z_{\text{EQ}}}$; and for $l \gtrsim \sqrt{1 + z_{\text{EQ}}}$ decreases as l^{-2} . In the case of non

scale-invariant tensor perturbations these results are modified by a factor of l^{nr} .

In Fig. 5 we show the tensor contribution to the angular power spectrum for no recombination and $z_{\text{LSS}} = 76$. The dramatic fall off occurs at a relatively small value of l , around 10. Thus, the tensor angular power spectrum can, in principle, be used to discriminate between standard recombination and no recombination, though due to cosmic variance, the finite ‘‘multipole resolution’’ of experiments, and the difficulty of separating the scalar and tensor contributions to CBR anisotropy this is by no means a simple task. The angular power spectrum also depends upon the deviation of the tensor perturbations from scale invariance, both in its amplitude relative to the scalar perturbations and its dependence upon l . The angular power spectrum for tilted tensor perturbations is shown in Fig. 6.

Finally, consider the cold dark matter + cosmological constant model (Λ CDM), proposed to reconcile a number of discrepancies of the CDM model with observational data [22]. It is characterized by: $\Omega_B \simeq 0.05$, $\Omega_{\text{cold}} \simeq 0.15$, $\Omega_0 = \Omega_B + \Omega_{\text{cold}} = 0.2$, $\Omega_\Lambda \simeq 0.8$, and $h \simeq 0.8$. For tensor perturbations most of the Sachs-Wolfe integral for the anisotropy arises near the last scattering surface where the effect of a cosmological constant is negligible. (This is not the case for scalar perturbations, and the formula for the Sachs-Wolfe contribution must be modified significantly [23].) Thus Eq. (23) for the contribution of tensor perturbations to the angular power spectrum is unchanged, with the following substitutions:

$$k_{\text{EQ}} = \frac{H_0 \sqrt{\Omega_0 / R_{\text{EQ}}}}{2\sqrt{2} - 2} \simeq 30H_0;$$

$$R_{\text{EQ}} = 4.18 \times 10^{-5} (\Omega_0 h^2)^{-1} \simeq 3.27 \times 10^{-4};$$

$$\begin{aligned}
\tau_0 &\simeq H_0^{-1} \int_0^1 \frac{dR}{\sqrt{\Omega_0 R + \Omega_0 R_{\text{EQ}} + \Omega_\Lambda R^4}} \simeq 3.89 H_0^{-1}; \\
\tau_{\text{LSS}} &\simeq 2\Omega_0^{-1/2} H_0^{-1} / \sqrt{1 + z_{\text{LSS}}} \simeq 0.135 H_0^{-1}.
\end{aligned}
\tag{38}$$

The angular power spectrum is shown in Fig. 7 for standard recombination in the Λ CDM model. Unfortunately, the difference between the Λ CDM and CDM models is not great.

Finally, it is also straightforward to modify our results for the energy density in gravitational waves today for the Λ CDM model:

$$\frac{d\Omega_{\text{GW}}}{d \ln k} = 4\Omega_0^2 \frac{V_{50}}{m_{\text{Pl}}^4} \frac{[\Gamma(\frac{3}{2} - \frac{1}{2}n_T)]^2}{(1 - \frac{5}{6}n_T)2^{n_T}[\Gamma(\frac{3}{2})]^2} (k/k_{50})^{n_T} |T(k/k_{\text{EQ}})|^2 (k/2H_0^{-1})^{-2}.
\tag{39}$$

Since the main change is to *reduce* the energy density on a given scale by a factor of $\Omega_0^2 \sim 0.04$, our conclusions about the direct detection of inflation-produced gravity waves remains.

We thank Paul J. Steinhardt for helping us make detailed comparisons between our work and that in Ref. [10]. This work was supported in part by the DOE (at Chicago and Fermilab) and by the NASA through NAGW-2381 (at Fermilab).

References

- [1] A.H. Guth and S.-Y. Pi, *Phys. Rev. Lett.* **49**, 1110 (1982);
A.A. Starobinskii, *Phys. Lett. B* **117**, 175 (1982); S.W. Hawk-

- ing, *ibid* 115, 295 (1982); J.M. Bardeen, P.J. Steinhardt, and M.S. Turner, *Phys. Rev. D* 28, 679 (1983).
- [2] V.A. Rubakov, M. Sazhin, and A. Veryaskin, *Phys. Lett. B* 115, 189 (1982); R. Fabbri and M. Pollock, *ibid* 125, 445 (1983); L. Abbott and M. Wise, *Nucl. Phys. B* 244, 541 (1984); B. Allen, *Phys. Rev. D* 37, 2078 (1988); L.P. Grishchuk, *Phys. Rev. Lett.* 70, 2371 (1993) and earlier references therein.
- [3] For a textbook discussion of inflation see e.g., E.W. Kolb and M.S. Turner, *The Early Universe* (Addison-Wesley, Redwood City, CA, 1990), Ch. 8.
- [4] R. Davis et al., *Phys. Rev. Lett.* 69, 1856 (1992); F. Lucchin, S. Matarrese, and S. Mollerach, *Astrophys. J.* 401, L49 (1992); D. Salopek, *Phys. Rev. Lett.* 69, 3602 (1992); A. Liddle and D. Lyth, *Phys. Lett. B* 291, 391 (1992); T. Souradeep and V. Sahni, *Mod. Phys. Lett. A* 7, 3541 (1992).
- [5] M.S. Turner, astro-ph/9302013 (FERMILAB-Pub-93/026-A).
- [6] Attempts at the reconstruction of the inflationary potential from observational data include, H.M. Hodges and G.R. Blumenthal, *Phys. Rev. D* 42, 3329 (1990); and more recently, E. Copeland, E.W. Kolb, A. Liddle, and J. Lidsey, FERMILAB-Pub-93/029-A (1993).
- [7] R.K. Sachs and A.M. Wolfe, *Astrophys. J.* 147, 73 (1967).

- [8] See e.g., G. Efstathiou, in *The Physics of the Early Universe*, eds. J.A. Peacock, A.F. Heavens, and A.T. Davies (Adam Higler, Bristol, 1990); J.R. Bond and G. Efstathiou, *Mon. Not. R. astron. Soc.* **226**, 655 (1987); J.R. Bond et al., *Phys. Rev. Lett.* **66**, 2179 (1991); P.J.E. Peebles, *Large-scale Structure of the Universe* (Princeton University Press, Princeton, 1980).
- [9] A.A. Starobinskii, *JETP Lett.* **11**, 133 (1985); L. Abbott and M. Wise, *Nucl. Phys. B* **244**, 541 (1984); M. White, *Phys. Rev. D* **46**, 4198 (1992); R. Fabbri, F. Lucchin, and S. Matarrese, *Phys. Lett. B* **166**, 49 (1986).
- [10] R. Crittenden et al., astro-ph/9303014; P.J. Steinhardt, private communication (1993).
- [11] B. Jones and R. Wyse, *Astron. Astrophys.* **149**, 144 (1985).
- [12] T.P. Walker et al., *Astrophys. J.* **376**, 51 (1991).
- [13] N. Tegmark and J. Silk, *Astrophys. J.*, in press (1993).
- [14] V.A. Rubakov, M.V. Sazhin, and A.V. Veryaskin, *Phys. Lett. B* **115**, 189 (1982); R. Fabbri and M. Pollock, *ibid* **125**, 445 (1983); B. Allen, *Phys. Rev. D* **37**, 2078 (1988); V. Sahni, *ibid* **42**, 453 (1990); M. White, *ibid* **46**, 4198 (1992).
- [15] G. Smoot et al., *Astrophys. J.* **396**, L1 (1992); E.L. Wright, *ibid* **396**, L3 (1992).
- [16] L. Krauss and M. White, *Phys. Rev. Lett.* **69**, 869 (1992).

- [17] M.S. Turner and F. Wilczek, *Phys. Rev. Lett.* **65**, 3080 (1990);
A. Kosowsky, Michael S. Turner, and R. Watkins *ibid* **69**, 2026
(1992).
- [18] J.M. Bardeen et al., *Astrophys. J.* **304**, 15 (1986).
- [19] D.H. Lyth and E.D. Stewart, *Phys. Lett. B* **274**, 168 (1992);
E.D. Stewart and D.H. Lyth, *ibid*, in press (1993).
- [20] D.R. Stinebring, M.F. Ryba, J.H. Taylor, and R.W. Romani,
Phys. Rev. Lett. **65**, 285 (1990).
- [21] A. Abramovici et al., *Science* **256**, 325 (1992); J. E. Faller et al.,
Adv. Space Res. **9**, 107 (1989).
- [22] M.S. Turner, G. Steigman, and L. Krauss, *Phys. Rev. Lett.* **52**,
2090 (1984); M.S. Turner, *Physica Scripta* **T36**, 167 (1991);
P.J.E. Peebles, *Astrophys. J.* **284**, 439 (1984); G. Efstathiou et
al., *Nature* **348**, 705 (1990).
- [23] K. Gorski, J. Silk, and N. Vittorio, *Phys. Rev. Lett.* **68**, 733 (1992).

FIGURE CAPTIONS

Figure 1: The qualitative behaviour expected for CBR anisotropy arising from scalar and tensor perturbations through the Sachs-Wolfe effect. The horizon-crossing amplitudes of the scalar and tensor perturbations are taken to be $\varepsilon_S \propto \lambda^{(1-n)/2}$ and $\varepsilon_T \propto \lambda^{-n_T/2}$ respectively (scale invariance corresponds to $n - 1 = n_T = 0$).

Figure 2: The evolution of the transfer function for gravity-wave perturbations; from top to bottom, the transfer function computed at red shifts $z = 0, 30, 100, 300, 1000$.

Figure 3: The energy density of the stochastic background of inflation-produced gravitational waves, in the scale-invariant limit (broken curve, arbitrary normalization), and for $n_T = -0.003, -0.03, -0.3$, normalized to the COBE DMR quadrupole (solid curves).

Figure 4: The tensor contribution to the angular power spectrum normalized to its quadrupole, and for reference the Sachs-Wolfe part of the scalar contribution normalized to its quadrupole (broken curve; note, for $l \gtrsim 100$ the Doppler and intrinsic contributions are more important than that of the Sachs-Wolfe). Tensor results are shown with (upper curve) and without (lower curve) the transfer function; in all cases $z_{\text{LSS}} = 1100$ and $h = 0.5$. (a) For $l \leq 100$; dotted curve shows tensor results with transfer function for $h = 1.0$. (b) For $l \leq 1000$.

Figure 5: The tensor contribution to the angular power spectrum normalized to its quadrupole, for $z_{\text{LSS}} = 76$ (solid curve) and for comparison $z_{\text{LSS}} = 1100$ (broken curve); in both cases $h = 0.5$.

Figure 6: Same as Fig. 4, except for non-scale invariant perturbations, $n - 1 = n_T = -0.15$. The results here correspond roughly to those in Fig. 4 “tilted” by a factor of $(l/2)^{-0.15}$.

Figure 7: The tensor contribution to the angular power spectrum normalized to its quadrupole for cold dark matter + cosmological constant with $z_{\text{LSS}} = 1100$, $\Omega_\Lambda = 0.8$, and $h = 0.8$ (solid curve) and for comparison, $z_{\text{LSS}} = 1100$, Ω_0 , and $h = 0.5$ (broken curve).

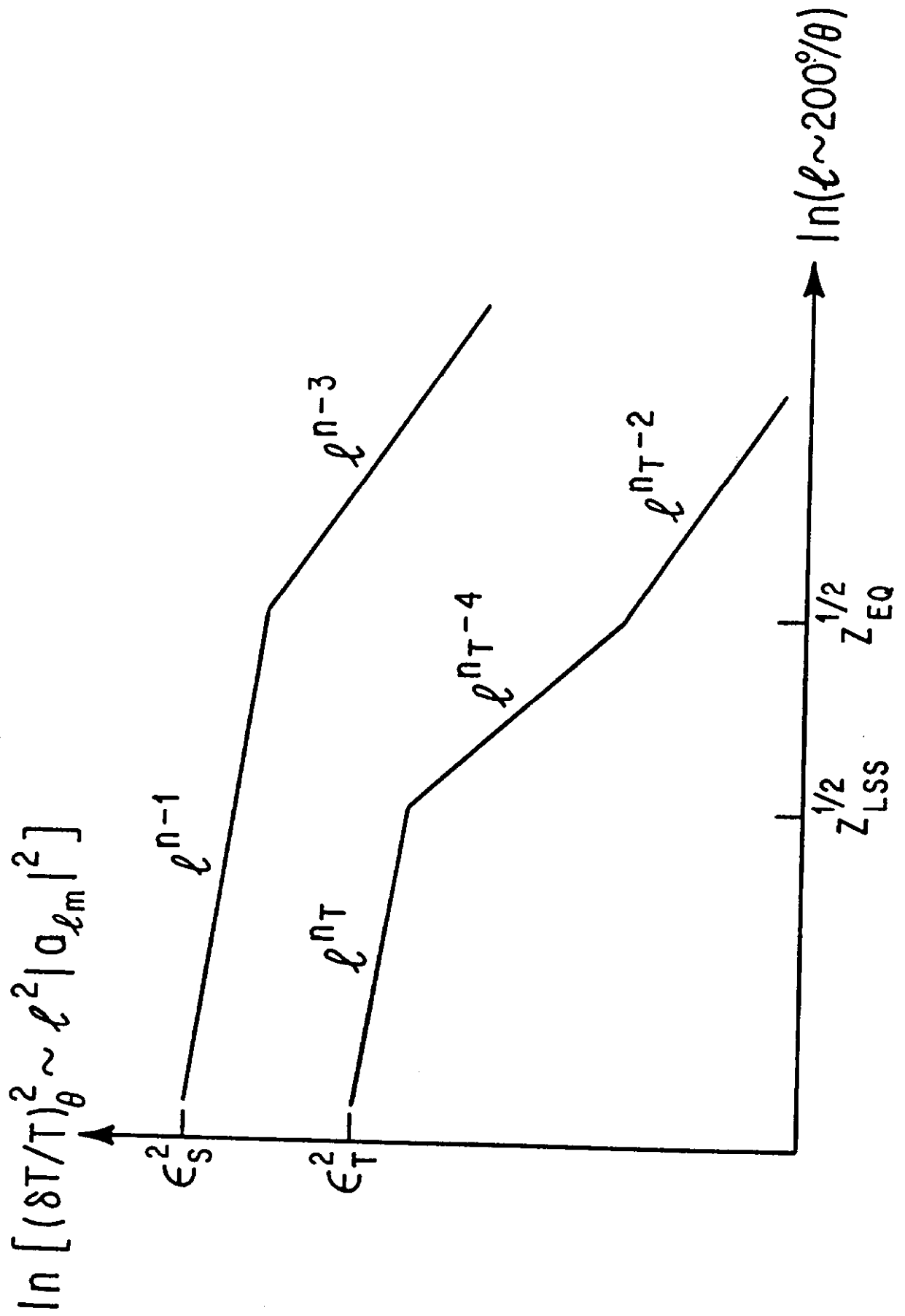


FIG 1

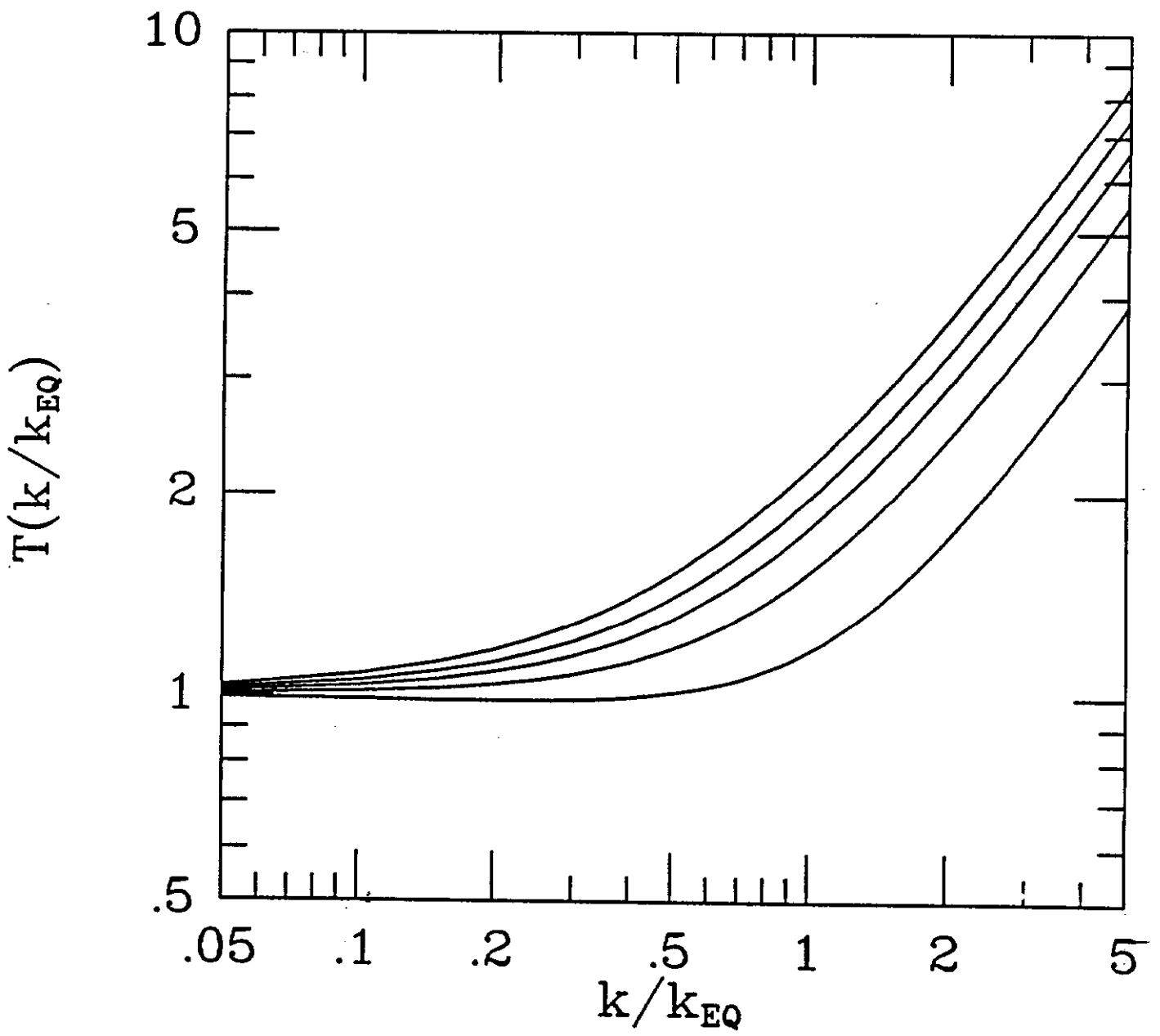


FIG 2

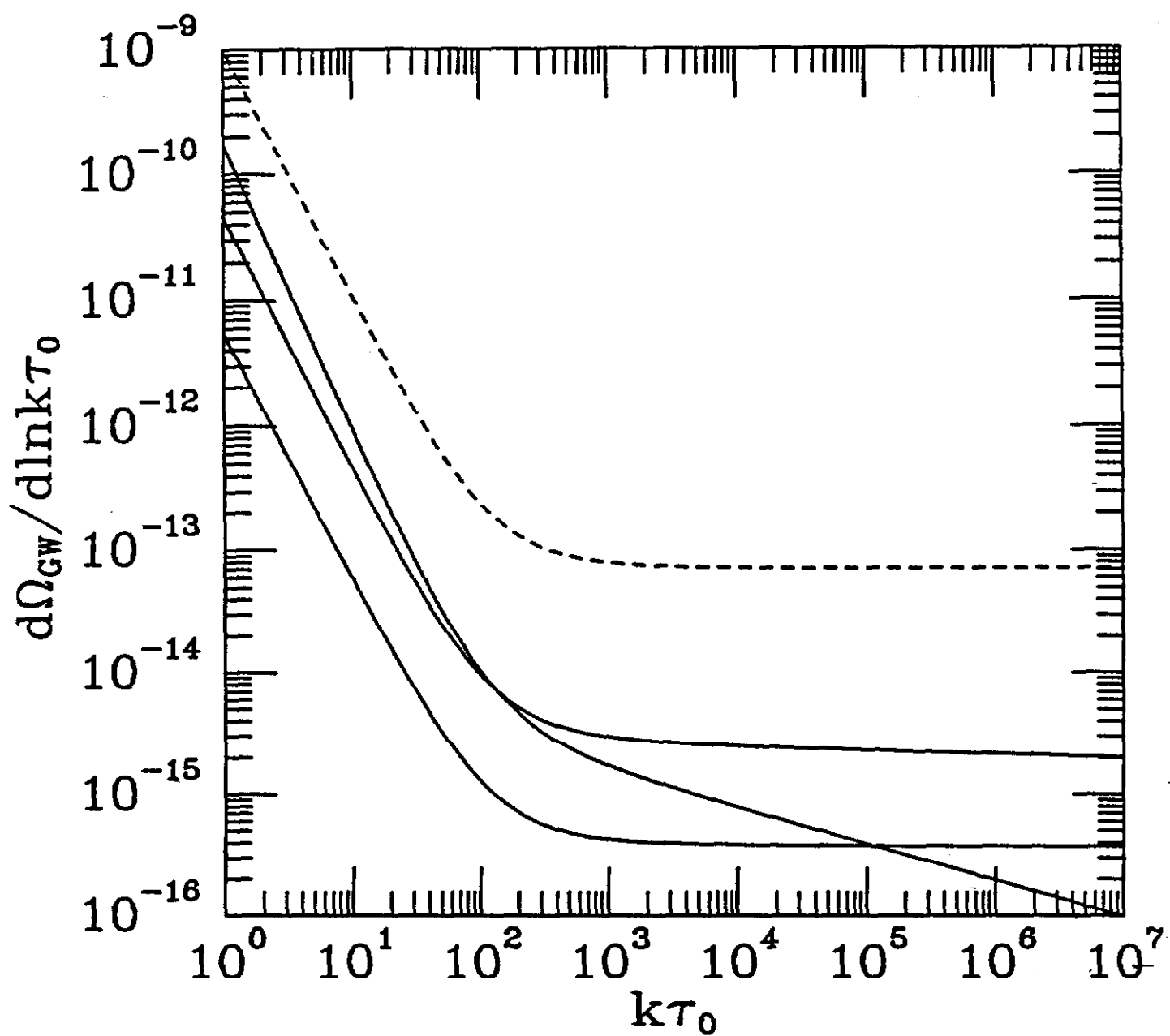


FIG 3

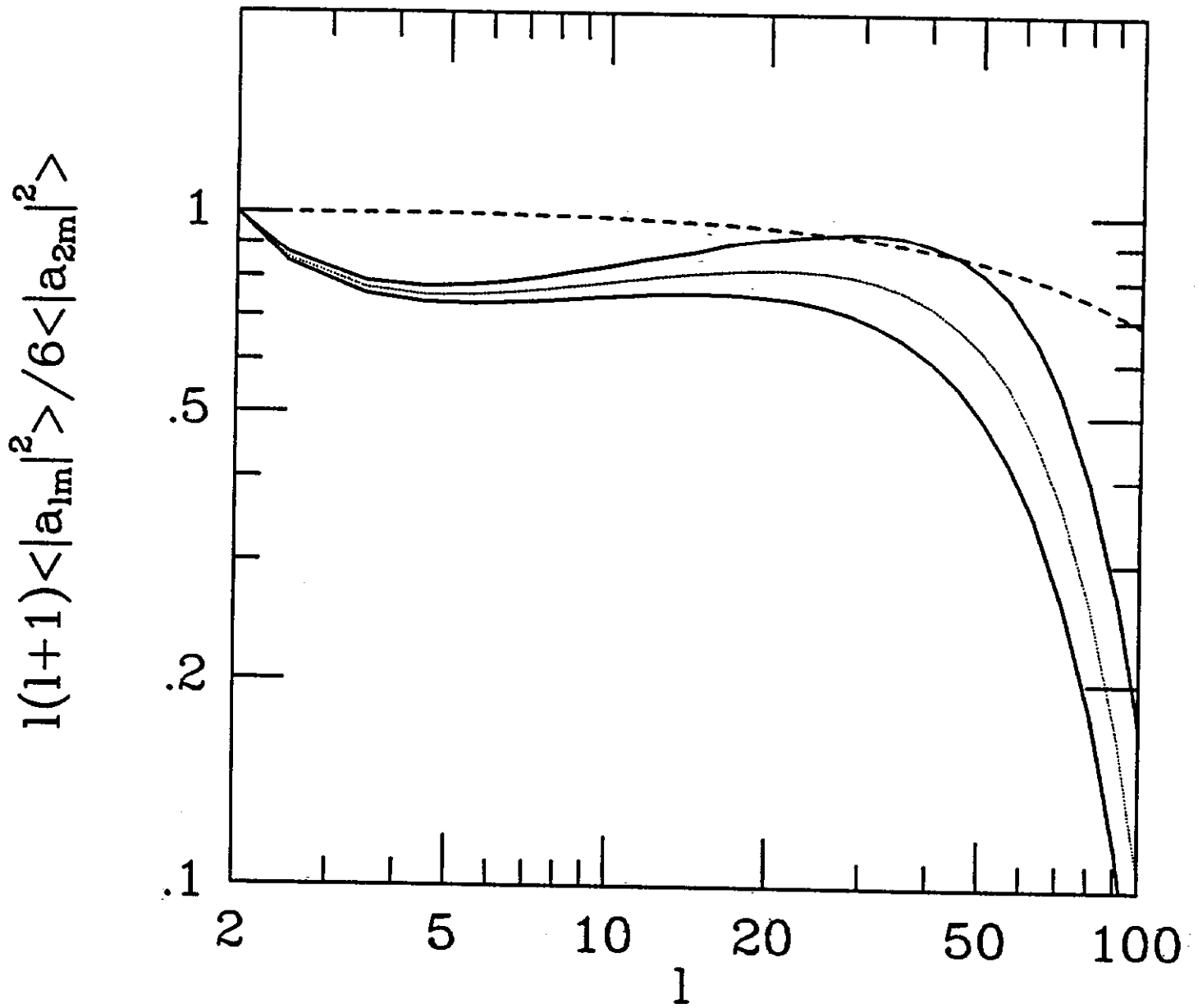


FIG 4a

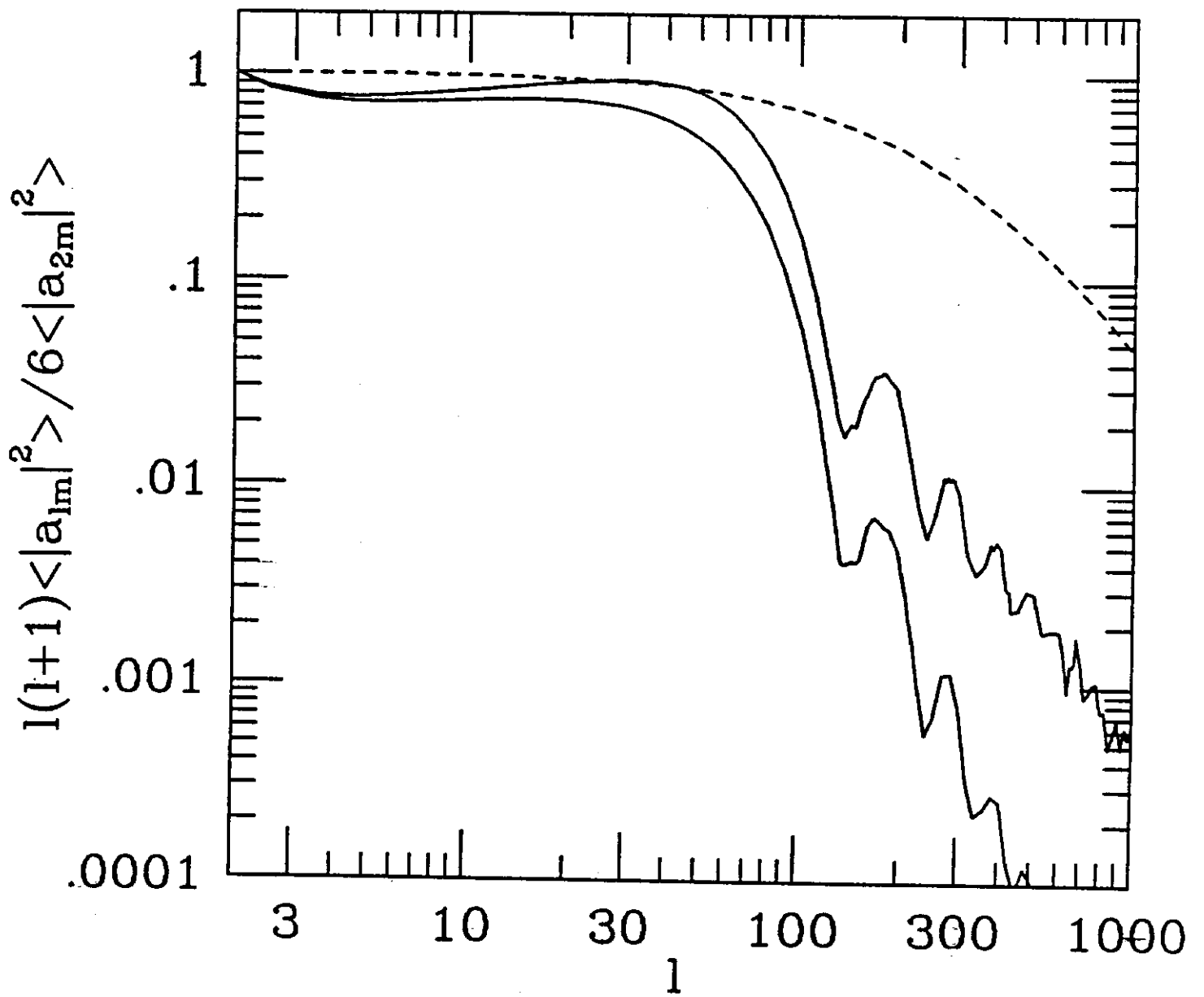


FIG. 4b

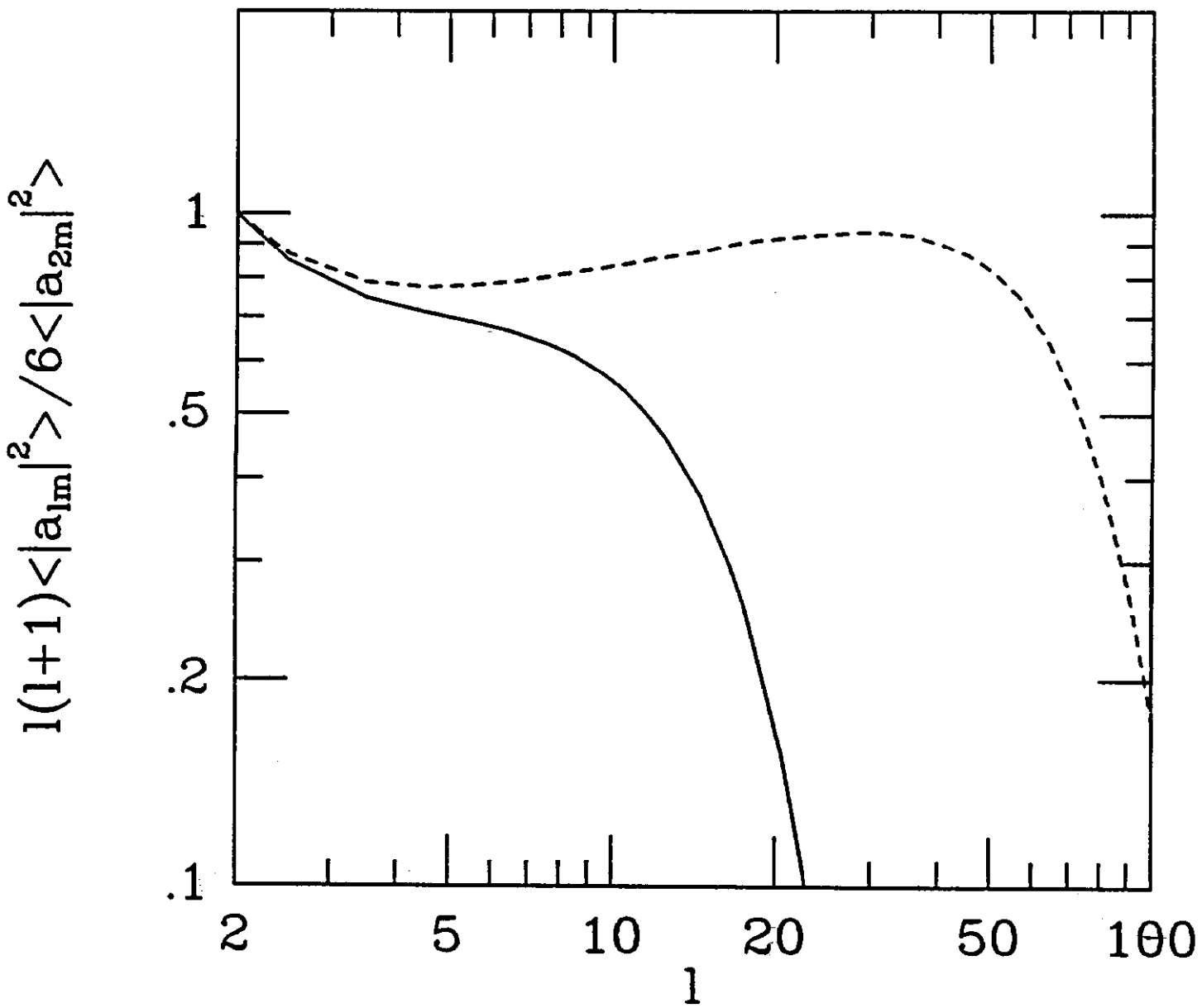


FIG 5